Intrinsic magnetic centers and microdomains in oxygen-deficient $YBa_2Cu_3O_{6.5}$ and $TmBa_2Cu_3O_{6+x}$

O. N. Bakharev,* L. K. Aminov, A. V. Dooglav,† A. V. Egorov, E. V. Krjukov, I. R. Mukhamedshin, V. V. Naletov,† M. A. Teplov, and A. G. Volodin
Magnetic Resonance Laboratory, Kazan State University, 420008 Kazan, Russia

J. Witteveen and H. B. Brom
Kamerlingh Onnes Laboratory, Leiden University, P.O. Box 9506, 2300 RA Leiden, The Netherlands

H. Alloul
Laboratoire de Physique des Solides, Université de Paris-Sud, 91405 Orsay Cedex, France
(Received 11 November 1996)

We measured the influence of magnetic centers (MC's) on the nuclear relaxation in 123 compounds using ^{169}Tm NMR and ^{63}Cu NQR in $TmBa_2Cu_3O_{6+x}$ ($x=0$, 0.2, 0.3, 0.4, 0.5, 0.6), and ^{89}Y NMR and ^{63}Cu NQR in $YBa_2Cu_3O_{6.5}$. Particular attention is paid to the region $0.5 \leqslant x \leqslant 0.6$ in order to deal with both a well-defined ortho II structure and a high enough MC concentration. The experiments reveal a two-component nuclear relaxation in the superconducting compounds at temperatures above 1 K, especially pronounced in the $x=0.5$ samples. The relaxation data give evidence for microphase separation due to oxygen disorder in the basal CuO_x planes. In the well-annealed samples, the MC's predominating the relaxation have $S=1/2$. The concentrations of these MC's are of the order of 3% in the disordered (nonsuperconducting) microphase and $\sim 0.3\%$ in the ordered (superconducting) one. [S0163-1829(97)07117-8]

I. INTRODUCTION

Oxygen-deficient $YBa_2Cu_3O_{6+x}$ compounds ($YBCO_{6+x}$) have a highly disordered crystal structure. Therefore, one might expect structural defects to give rise to a rich variety of magnetic defects, i.e., magnetic centers (MC's) like Cu^{2+} and Cu^{3+} ions or paramagnetic copper-oxygen clusters. Electron paramagnetic resonance (EPR) is the most powerful experimental method for studying the structure and energy spectra of MC's in solids.[1] However, as EPR signals from paramagnetic copper ions and/or copper-oxygen clusters are absent in $YBCO_{6+x}$ superconductors with $x<0.7$ and $x>0.9$,[2,3] EPR studies on high-T_c superconductors are much less effective than on solid insulators and normal metals. The absence of an EPR signal does not mean that the 123 superconductors do not contain intrinsic MC's at all. Specific heat measurements on a variety of $YBCO_{6+x}$ samples[4] show that the volume fraction of superconductivity is strongly sample dependent and that the nonsuperconducting (NSC) regions are associated with a low concentration of Cu^{2+} magnetic moments, which are present even in well-oxygenated (and well-ordered) compounds.

Nuclear magnetic resonance (NMR) and nuclear quadrupole resonance (NQR) are excellent alternative tools for the investigations of MC's in solids. At low temperature (T) the nuclear spin-lattice relaxation (NSLR) in insulators can only proceed via impurity MC's well coupled to phonons.[5] The same conditions should hold in high-T_c superconductors at temperatures well below T_c, where the relaxation mechanism due to interaction between nuclear spins and conduction electrons (holes) becomes ineffective. When studying nuclear relaxation via impurity paramagnetic ions in dielectric crystals using the spin echo method, the strength of the rf field H_1 often exceeds the resonance linewidth $\Delta\omega$: $\gamma H_1 > \Delta\omega$ in order to influence all nuclear spins of the sample by the rf field. If the nuclear spin I is equal to 1/2 and there is no inhomogeneous broadening of the NMR line, the uniform nuclear spin polarization establishes rather fast after the rf pulse due to efficient nuclear spin diffusion; in this case the recovery of the longitudinal nuclear magnetization after the saturating pulse has a simple exponential time dependence $\exp(-t/T_1)$, characterized by a single parameter T_1. If the NSLR is then caused by MC's, their concentration can be determined from the T_1 data, but it is usually impossible to fix their location or the distribution in the crystal lattice.

In high-T_c superconductors the location of intrinsic MC's and their relation with structural defects is of main interest. As shown in Secs. IV, V, and the Appendix, one can obtain the desired information taking as a probe those nuclei, of which the resonant lines are strongly inhomogeneously broadened by the defects. In that case $\gamma H_1 < \Delta\omega$, and the kinetics of longitudinal nuclear magnetization recovery becomes nonexponential, while the shape of the recovery curve appears to be dependent on the distribution of the MC acceptors in the crystal lattice. The analysis of nonexponential magnetization recovery curves is rather complicated, but in the simplest case when the nuclear resonance spectrum consists of single inhomogeneously broadened line, the analysis appears to be possible and useful.

Thus the right choice of the probe nucleus with the appropriate NMR-NQR spectrum is very important. In

$YBCO_{6+x}$ compounds copper nuclei with $I=3/2$, the NQR spectrum which consists of one line broadened mainly by differences in the crystal electric field gradient, serve as such probe. In $TmBCO_{6+x}$ compounds the nuclei of the $^{169}Tm^{3+}$ ions are also useful (nuclear spin $I=1/2$, 100% natural abundance).[6] The Tm^{3+} ground state of the $4f$-electron shell in the crystal electric field of $TmBCO_{6+x}$ is a singlet separated from the excited Stark sublevels by an interval of more than 150 K. The peculiar property of Tm nuclei in such a so-called ''Van Vleck paramagnet'' is that they have a well-defined enhanced nuclear magnetic moment.[7] This moment is very sensitive for small variations in the local surrounding of the $^{169}Tm^{3+}$ ions in the $TmBCO_{6+x}$ lattice, so that the thulium NMR line observed at low temperatures is strongly broadened, even in the $x=0$ or $x=1$ samples which are usually considered to be crystallographically perfect. Like ^{89}Y the ^{169}Tm nuclei make up the main crystal lattice and reside between the CuO_2 layers responsible for the superconductivity. The Tm probe can only be used below 10 K, because at $T>10$ K thermally induced fluctuations of the hyperfine magnetic fields from the $4f$-electron shell provide the main relaxation mechanism. At temperatures above 10 K, ^{89}Y can be used as probe instead.

The NSLR rates of ^{169}Tm nuclei in the series of $TmBCO_{6+x}$ samples ($0<x<1$) at temperatures below 4.2 K have clearly shown[8–10] that thulium nuclei relax via intrinsic MC's, of which the concentration depends strongly on the oxygen content and reaches a maximum value of ~ 0.07 per unit cell at the ''semiconductor-superconductor'' transition ($x=0.4$). Further investigations of the ^{169}Tm NMR in the quenched oxygen-deficient $TmBCO_{6.5}$ and $TmBCO_{6.6}$ samples at temperatures from 4.5 K down to 0.7 K have revealed that the MC's with a concentration maximum at $x=0.4$ are likely located in the CuO_2 planes.[11] The principal Tm NMR features in oxygen-deficient superconducting (SC) $TmBCO_{6+x}$ are as follows.[8–10,12] In well-annealed samples the Tm NSLR kinetics obeys the relation

$$1-M_t/M_\infty=\exp[-(t/T_1)^m]\exp(-t/T_1'), \tag{1}$$

with M_t the magnetization at time t, and T_1 and T_1' the NSLR times. The value of m equals 1/2, which is typical for a three-dimensional (3D) distribution of impurity MC's in a crystal lattice (see the Appendix). $1/T_1'$ of the Tm nuclei at liquid helium temperatures has nonzero values ($\sim 1\ s^{-1}$) only in the overdoped samples ($x>0.94$). Equation (1) with $m=1/2$ is a particular case of ''Förster law,'' and is known to be valid in the absence of the nuclear spin diffusion,[13,14] when nuclear spins relax directly via MC's randomly distributed in a crystal lattice. The diffusionless relaxation of Tm nuclei in $TmBCO_{6+x}$ can be easily understood, since the numerous crystal lattice defects result in large differences between the local crystal electric fields and, consequently, between the Larmor frequencies of the Tm nuclei.[15]

The same crystal lattice defects are responsible for the distortions of the electric field gradients at the copper sites, resulting in a diffusionless relaxation of Cu nuclei in oxygen-deficient compounds.[16]

According to EPR data[2,17–19] the most widespread MC's in oxygen-deficient 123 compounds are those with $S=1/2$ and typical g values $g_\parallel=2.3\pm0.08$ and $g_\perp=2.05\pm0.03$. In the case of diffusionless relaxation via MC's with $S=1/2$ the nuclear magnetization can be anticipated to recover according to Eq. (1) with $m=D/6$ (see the Appendix). The NSLR rate depends on the MC parameters as follows:

$$1/T_1^{(D)}=A_D\frac{\tau_c}{1+\omega_0^2\tau_c^2}(1-P_0^2). \tag{2}$$

Here D is a dimensionality of the MC distribution, ω_0 is the nuclear resonance frequency, τ_c is a correlation time for the local magnetic field fluctuations produced by MC's at the nuclear sites, $P_0=\tanh(g\mu_B H/2kT)$ is the MC polarization factor. The coefficient $A_D\sim n^{6/D}$ depends on n and D (i.e., on the location of MC's in the crystal lattice), and on the strength of dipolar interaction between nuclei and MC's. In general, the correlation time τ_c is determined by the MC's spin-lattice (τ_1) and spin-spin (τ_2) relaxation times,[5]

$$1/\tau_c=1/\tau_1+1/\tau_2. \tag{3}$$

If the spin-spin relaxation time τ_2 (independent of temperature) is much shorter than τ_1, the T dependence of the NSLR rate is entirely determined by the factor $(1-P_0^2)$. This makes it possible to estimate the effective g values of MC acceptors from T_1 at low temperatures and thus to distinguish between different types of MC's.

In this paper we clarify the origin of the MC's in 123 compounds using ^{169}Tm NMR and ^{63}Cu NQR in $TmBCO_{6+x}$ ($x=0$, 0.2, 0.3, 0.4, 0.51, 0.6), and ^{89}Y NMR and ^{63}Cu NQR in $YBCO_{6.5}$. Particular attention is paid to the x region of 0.5–0.6 in order to deal with both a well-defined ortho II structure and a high enough MC concentration. The experiments reveal a two-component nuclear relaxation in the SC compounds at temperatures above 0.7 K, especially pronounced in the $x=0.5$ samples. The relaxation data are interpreted as evidence for microphase separation due to oxygen disorder in the basal CuO_x planes. The kinetics of the nuclear relaxation in both microphases are shown to be of the $m=1/2$-type with relaxation rates differing by a factor of 10–20. The nuclear relaxation process exibits a typical temperature dependence $T_1^{-1}\sim(1-P_0^2)$, down to $T_s\sim 0.7$ K, at which point some kind of a spin-glass transition takes place. At temperatures below T_s (down to $\sim$ 0.1 K) the nuclear relaxation in both microphases of the superconductor with $x=0.5$ follows the law $T_1^{-1}\sim T^p$ ($p\approx 2$) similar to that observed in the nonsuperconducting compounds with $x=0$ and 0.2.[20]

The rest of the paper is arranged as follows. Experimental details are given in Sec. II, followed by a description in Sec. III of the $^{63}Cu(1)$ NQR and ^{89}Y NMR in $YBCO_{6.5}$. Special attention is paid in Sec. III to changes in both nuclear relaxation times (T_1) and critical temperatures (T_c) produced by room-temperature annealing (RTA) of quenched $YBCO_{6.5}$. In Sec. IV the available experimental data[11] on the ^{169}Tm relaxation in quasiequilibrium ($t_{RTA}=2$ weeks) samples of $TmBCO_{6+x}$ ($x=0.5$, 0.6) are reanalyzed on the basis of microphase separation. Via computer simulation of the Tm nuclear magnetization recovery curves for 1.0 K $<T<$ 4.5 K information is obtained about the intrinsic MC's such as location, concentration, probability of direct transfer of a nuclear spin excitation to a MC acceptor, and splitting of

MC energy levels in a magnetic field. The experimental data on the ^{63}Cu(1) and ^{169}Tm relaxation in well-annealed (and well-ordered) powder samples of $TmBCO_{6+x}$ ($0<x<0.6$) aligned in a magnetic field are presented and analyzed in Sec. V. Again, a computer simulation analysis is used to obtain information on the spin-spin interactions responsible for the nuclear relaxation at low temperatures.

II. EXPERIMENT

MC's in 123 compounds are, most likely, induced by crystal lattice defects, such as oxygen vacancies. For that reason, we studied the NMR-NQR spectra and the nuclear relaxation rates at low temperatures using samples, that were quenched in liquid nitrogen and thereafter annealed at room temperature (RTA) for a time interval t_{RTA}. The nonequilibrium samples were prepared from the starting ceramic materials with $0.90<x<0.95$ by annealing in air at temperatures T_a of 1000 ± 25 K during a time $t_0>1$ h followed by fast quenching in a liquid nitrogen. The oxygen content of quenched samples was estimated using the relation $6+x=7.44-1.27\times10^{-3}T_a$.[21] The oxygen diffusion coefficient at temperatures above 975 K exceeds 10^{-9} cm^2/s.[22] Therefore, the diffusion length $2(Dt_0)^{1/2}$ for $t_0>1$ h is expected to be much greater than the maximum grain size of the starting materials ($\sim$ 10 μm), resulting in a homogeneous distribution of oxygen in the samples. After high T annealing all samples were as rapidly as possible (<1 s) quenched in liquid N_2. Two ''nonequilibrium'' powdered $YBCO_{6+x}$ samples denoted as Cu6.5 and Y6.5, were studied (see Sec. III) with t_{RTA} varying from minutes to 8 months. Another two ''quasiequilibrium'' $TmBCO_{6+x}$ samples with $x=0.5$ and 0.6, denoted (see Sec. IV) as Tm6.5-*qe* and Tm6.6-*qe*, were obtained by annealing at room temperature for $t_{\mathrm{RTA}}=2$ weeks. In addition, six ''equilibrium'' $TmBCO_{6+x}$ samples with $x=0$, 0.2, 0.3, 0.4, 0.51, and 0.6, denoted (see Sec. V) as Tm6.0, Tm6.2, Tm6.3, Tm6.4, Tm6.5, and Tm6.6, respectively, were studied in the present experiments. These samples (well annealed, mixed with paraffin, and aligned in a magnetic field) were studied previously,[8–10] and up to the present measurements they were kept at room temperature for 4 y after preparation.

Tm6.5-qe and Tm6.6-qe nonaligned powders mixed with Teflon oil were studied by ^{169}Tm NMR at frequencies ν of 90 MHz and 125 MHz, Y6.5 mixed with paraffin oil by ^{89}Y NMR at $\nu=15.6$ MHz, and Cu6.5 freely packed as a ''dry powder'' by ^{63}Cu(1) NQR at $\nu=31.5$ MHz and ^{89}Y NMR at $\nu=19.6$ MHz. The series of well-annealed $TmBCO_{6+x}$ samples was studied by ^{169}Tm NMR and ^{63}Cu(1) NQR at the fixed frequency of 31.55 MHz. The diamagnetic susceptibility of nonequilibrium samples vs RTA time was measured using either a low frequency bridge (for Y6.5 and Cu6.5) or a SQUID magnetometer (for Tm6.5-*qe* and Tm6.6-*qe*). The values of T_c of the samples exposed to rather long RTA ($t_{\mathrm{RTA}}>2$ weeks) were used for an independent estimation of x on the basis of the T_c vs x dependences previously reported by Bakharev *et al.*[9] and by Graf *et al.*[23] All the relaxation measurements were performed with homebuilt pulsed NMR-NQR spectrometers. In the experiments with $TmBCO_{6+x}$ compounds the temperatures from 1.2 K down to 0.7 K were obtained in a ^{3}He cryostat, at lower temperatures a ^{3}He-^{4}He dilution refrigerator was used.

III. ^{63}Cu(1) NQR AND ^{89}Y NMR IN $YBa_2Cu_3O_{6.5}$

Already in the first papers devoted to Tm NMR (Refs. 8–10) it was mentioned that the MC acceptor concentration approximately scales with the concentration of pairs of ''terminating'' $Cu^{2+}(1)$ ions in CuO chains, and it was concluded that MC acceptors are located at the boundaries between SC and NSC domains. Applied to the oxygen-deficient equilibrium 123 compounds, for which mesoscopic phase separation (structural or ''chemical'') is typical, the latter conclusion looks quite probable but nevertheless needs additional confirmation. The $Cu(1)_2$ nuclei located in ''empty'' Cu–$\cdots$–Cu chains (i.e., twofold coordinated by oxygen) seem to be good probes because a distinct (clearly ''resolved'') line referring to the SC domains of the ortho II phase is observed in the NQR spectrum of copper in these samples. Along with this line there are lines in the $Cu(1)_2$ NQR spectrum which do not refer to the ortho II phase domains, which allows a comparison of relaxation characteristics of different $Cu(1)_2$ centers located at different sites of the mesoscopically disordered crystal structure. Another advantage of Cu(1) nuclei as a probe is the possibility to use them in the absence of the external magnetic field. At sufficiently low temperature this allows the detection of the lowest energy excitations of the intrinsic magnetic defects and possible magnetic phase transformations in the oxygen-deficient 123 compounds.

Below we describe the results of $^{63}Cu(1)_2$ nuclear relaxation studies of the $YBCO_{6.5}$ quenched samples ''aged'' at room temperature for the time t_{RTA} from 6 min up to 8 months. The NQR spectrum of twofold coordinated $^{63}Cu^{+}(1)$ atoms consists of three lines[24] observed at the frequencies 31.5 MHz (these type-*A* copper centers belong to the ''empty'' Cu-Cu chains residing between two ''filled'' Cu–O–$\cdots$–O–Cu chains), 30.9 MHz (type-*B* centers, one of the neighboring chains is empty), and 30.3 MHz (type-*C* centers, both neighboring chains are empty). As one can see in Fig. 1(a), in quenched Cu6.5 the *B*-type line has a maximum intensity. Room-temperature annealing increases the intensity of line *A*, corresponding to the ordered ortho II phase, at the expense of the intensity of line *B*. The ^{63}Cu(1) NQR spectra for well-annealed $TmBCO_{6+x}$ samples studied earlier[8–10] are shown for comparison in Fig. 1(b). These spectra visualize the formation of the ordered ortho II phase.

The increase of T_c by annealing of Cu6.5 at room temperature is given by

$$T_c(t)=T_c(\infty)-[T_c(\infty)-T_c(0)]\exp(-t/\tau_{\mathrm{RT}}^{(1)}) \qquad (4)$$

with a characteristic time $\tau_{\mathrm{RT}}^{(1)}=22$ h [solid line in Fig. 2(a)]. The Cu(1) NSLR for $T<15$ K is described by Eq. (1), in which $1/T_1'=0$ and $m\approx1/3$ for all annealing times t_{RTA} up to 8 months. The increase of T_1 during annealing reflects the decrease of MC's and proceeds according

$$T_1(t)=T_1(\infty)-[T_1(\infty)-T_1(0)]\exp(-\sqrt{t/\tau_{\mathrm{RT}}^{(2)}}), \qquad (5)$$

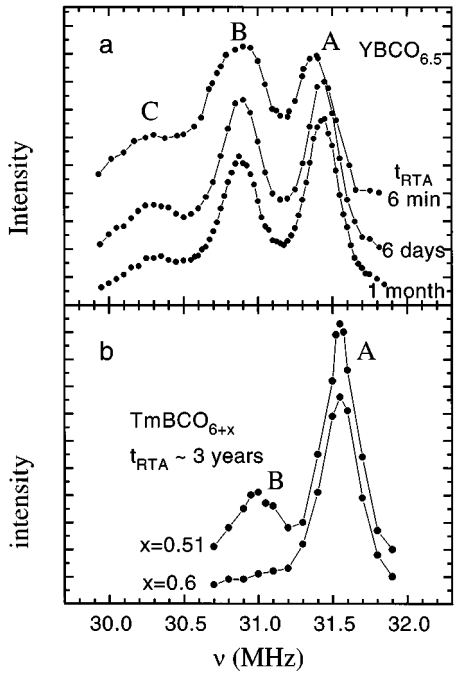

FIG. 1. (a) ^{63}Cu(1) NQR spectra in nonequilibrium $YBCO_{6.5}$ at $T=4.2$ K; (b) ^{63}Cu(1) NQR spectra in well-annealed $TmBCO_{6+x}$ at $T=4.2$ K. Lines *A*, *B*, and *C* correspond to three kinds of Cu(1) centers (see text).

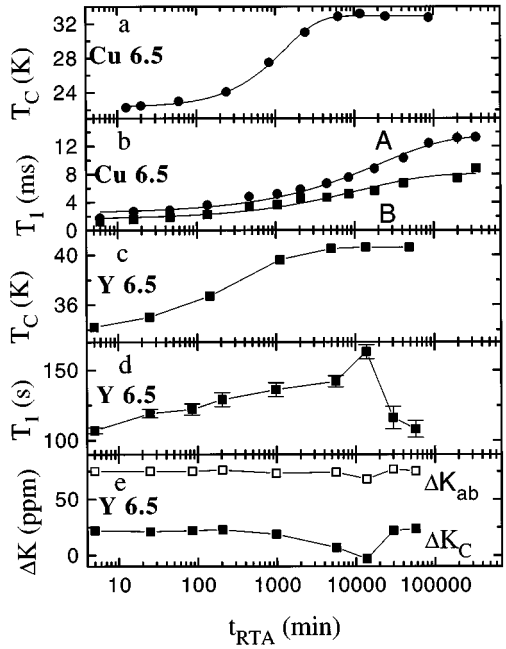

FIG. 2. Characteristic parameters of Cu6.5 and Y6.5 vs t_{RTA}. (a) T_c of Cu6.5; (b) ^{63}Cu(1) T_1 in Cu6.5 at $T=4.2$ K at 31.5 MHz (*A* line) and 30.9 MHz (*B* line); (c) T_c of Y6.5; (d) ^{89}Y T_1 in Y6.5 at $T=100$ K at 15.64 MHz; (e) ^{89}Y NMR shifts in Y6.5 at $T=100$ K as deduced from the powder spectra (Fourier transforms of the spin echo signal).

with $\tau_{RT}^{(2)}=270$ h [Fig. 2(b)] exceeding $\tau_{RT}^{(1)}$ by one order of magnitude. It should be noted that the kinetics given by Eq. (5) has been used earlier[25,26] for fitting the dependence of T_c on t_{RTA}. Assuming $1/T_1 \sim n^3$ (see the Appendix) we can conclude from Fig. 2(b) that an annealing period of 8 months of room temperature compared to a $t_{RTA}=6$ min gives only 40% less MC's.

The T dependences of $1/T_1$ for the *A* and *B* lines in Cu6.5 ($t_{RTA}=2$ months) are presented in Fig. 3. As is seen, in a wide T range down to 0.08 K the relaxation rate of the *B* nuclei is approximately 1.5–2 times higher than that of the *A* nuclei supporting the idea that MC's are located outside the ortho II domains. In the narrow T range from 4.2 K down to 2.2 K the ^{63}Cu NSLR rates at both *A* and *B* lines in Cu6.5 reveal a nonmonotonous dependence on T, the difference between $T_1^{-1}(A)$ and $T_1^{-1}(B)$ becoming negligible. At the moment, we cannot find a satisfactory explanation for such T_1^{-1} vs T behavior. At lower temperatures (from 2 K down to 0.08 K) the $T_1^{-1}(A)$ and $T_1^{-1}(B)$ values appear to differ again by a factor of ~ 2, and at temperatures below 1 K $T_1^{-1} \sim T^{1.5}$ for both *A* and *B* lines (see straight lines in Fig. 3). A similar T dependence of a NSLR rate has been observed earlier[27] for ^{139}La nuclei in AF $La_{2-x}Sr_xCuO_4$ ($x \leqslant 0.018$) at temperatures below $T_f=x(815\ \mathrm{K})$, where the freezing of the effective spin degrees of freedom of the doped holes was concluded to take place resulting in a spin-glass-like state. The appearance of the spin-glass-like behavior of our $YBCO_{6.5}$ superconducting sample can be apparently associated with the magnetic boundaries (walls) separating mesoscopic domains of the ortho II phase.

The ^{89}Y NMR in the Y6.5 sample was studied at $T=100\ \mathrm{K} > T_c$. The experimental conditions did not differ from those described earlier.[28] T_c, the ^{89}Y NSLR time T_1 (the usual exponential recovery was observed at all t_{RTA} times) and the ^{89}Y NMR shifts as functions of t_{RTA} are shown in Figs. 2(c)–2(e). At the end of the annealing procedure ($t_{RTA}=40$ days) the ^{89}Y NMR parameters appear to be

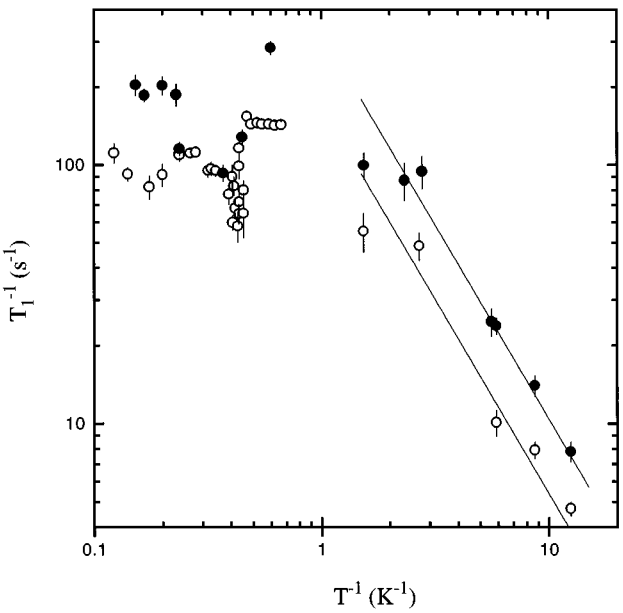

FIG. 3. T dependences of ^{63}Cu(1) $1/T_1$ in Cu6.5 ($t_{RTA}=2$ months) at 31.5 MHz (*A* line, open circles) and 30.9 MHz (*B* line, solid circles). Straight lines for $T^{-1} > 0.7\ \mathrm{K}^{-1}$ correspond to $T_1^{-1} \propto T^{1.5}$.

the same as those in the quenched sample, whereas T_c becomes 6 K higher. These ''final'' quantities, $10^3/T_1T=0.09\ \mathrm{s}^{-1}\,\mathrm{K}^{-1}$, $\Delta K_{ab}=75$ ppm, $\Delta K_c=22$ ppm, agree with those obtained earlier,[28] and shows the reliability of the following experimental findings: (i) the maximum value of T_c is reached after 10-day annealing of the quenched $YBCO_{6.5}$ sample at room temperature; (ii) during these 10 days, the ^{89}Y T_1 first increases for 50%, and then decreases returning to the value characteristic for the as-quenched sample. These results are in accordance with previous findings[29] that for the chain-plane oxygen rearrangement process connected to the *T-O* transition thermodynamic equilibrium is obtained by an annealing period of about 1 week at room temperature.

The correlations between T_c vs t_{RTA} in Figs. 2(a) and 2(c) and T_1 vs t_{RTA} in Fig. 2(b) (the latter for $t_{\mathrm{RTA}}\leqslant 10\,000$ min) indicate that in the course of RTA ordering of charges and spins takes place in the copper-oxygen layers and that this process becomes completed, mainly during the first 10 days. This ordering process is most likely governed by an oxygen ordering process in CuO_x basal planes. Indeed, if the mean time t_d of a diffusive transfer of an oxygen atom from the O(5) position to the ''chain'' O(1) position equals 30 min at room temperature,[30] then during 10 days the oxygen atoms undergo approximately 500 such displacements. As a result of this diffusive motion, a certain type of mesoscopic structure like the ''secondary tweed ortho II''[31] appears in the CuO_x basal planes. According to our estimates,[8] the mean length of CuO chain fragments in $x=0.5$ compounds does not exceed the value of $6b_0$ even in well-annealed samples. Since 60–70 elementary O(5)–O(1) displacements are needed to form the mesoscopic ortho II domains of $6b_0$ size,[31] the quantity $500t_d$ can be interpreted as the time interval needed for forming structurally correlated (in the *c* direction) ortho II domains in adjacent CuO_x layers. A direct connection between ordering processes in CuO_2 and CuO_x layers follows from these estimates. Moreover, superconductivity in 123 systems is possible even in the absence of a structural correlation between CuO_x planes (at small t_{RTA}), although such correlations seem to be necessary for reaching a maximum T_c.

The acceleration of Y nuclear relaxation during further annealing ($t_{\mathrm{RTA}}=10$ days$\rightarrow$40 days) is hardly connected with the appearance of some new MC's in the sample (their appearance should be ''noticed'' by other nuclei). The explanation should most likely be looked for in the increase of the charge carrier concentration in the CuO_2 planes and/or its redistribution between the layers of the non-single-phase system. An additional study of T_1^{-1} vs t_{RTA} dependence for Y nuclei is needed to clearly distinguish between the contributions to the relaxation related with AF fluctuations arising from the CuO_2 planes in the ''perfect'' material and local field fluctuations from intrinsic MC's of the $YBCO_{6+x}$ lattice.

In addition to this study above T_c, we also checked the T dependence of the ^{89}Y T_1 in Cu6.5 down to 4.2 K in a field of 94 kOe. After an initial Korringa-like increase from 26 s at 300 K to 160 s at 60 K T_1 drops to a plateau value of 60 s below 20 K. Below 20 K, where the line is severely broadened by the flux lattice, the recovery becomes strongly nonexponential. The absolute value of 60 s compares reasonably well with the Tm values (10 ms in 6 kOe)[11] in the same temperature interval, if the differences in gyromagnetic ratios [$\gamma_a(\mathrm{Tm})/\gamma(\mathrm{Y})\sim 26$] and aging time of the sample are taken into account.

IV. ^{169}Tm NUCLEAR RELAXATION IN QUASIEQUILIBRIUM $TmBa_2Cu_3O_{6+x}$ COMPOUNDS

Although the critical temperature T_c of the quenched samples with $x=0.5$ reaches its maximum just after 10 days of room temperature annealing [see Fig. 2(a) and 2(c)], spin and charge ordering in copper-oxygen planes continues to go on. Obviously, this can be seen from the yttrium spinlattice relaxation, but because these times are very long at low temperatures, the thulium nucleus is a much more suitable ''interlayer'' probe at liquid helium temperatures. Below we analyze T_1 in the Tm6.5-*qe* and Tm6.6-*qe* samples, called ''quasiequilibrium'' because of rather short annealing ($t_{\mathrm{RTA}}=20\,000$ min, cf. Fig. 2).

The Tm spectra in $TmBCO_{6+x}$ are described[6] by the Hamiltonian $\mathcal{H}=-\hbar\Sigma\gamma_\lambda H_\lambda I_\lambda$, whose parameters $|\gamma_b/2\pi|$ and $|\gamma_c/2\pi|$ at temperatures below 4.2 K have the following values: 6.8(1) and 2.20(5) kHz/Oe in the ortho I phase ($x=1$), 6.1(1) and 2.56(5) kHz/Oe in the ortho II phase ($0.5<x<0.6$), and 5.3(1) and 3.05(5) kHz/Oe in the tetragonal phase ($x=0$). The particular feature of these spectra is that the parameter $|\gamma_a/2\pi|=5.3(1)$ kHz/Oe does not depend on x; therefore, at the condition $H=\omega/\gamma_a$, fulfilled in the relaxation measurements on nonaligned powders, similar parts of the Tm nuclei gave a resonant response to the radio-frequency pulses. The Tm relaxation studies of sample Tm6.6-*qe* at frequencies of 90 and 125 MHz have revealed the $\exp[-(t/T_1)^{1/2}]$-type kinetics in the temperature range from 0.7 to 4.2 K indicating a 3D character of a MC distribution in a crystal lattice. In contrast, the $\exp[-(t/T_1)^{1/3}]$-type kinetics was found for Tm6.5-*qe* at temperatures above 2 K transforming into the $\exp[-(t/T_1)^{1/2}]$-type at $T<1$ K, which has been interpreted as evidence for quasi-2D distribution of the singlet-ground-state MC's located at short distances from the Tm ions, i.e., localized in the CuO_2 planes.[11]

Although we do not exclude the probable presence of the singlet-ground-state copper-oxygen clusters in the CuO_2 planes of the quenched materials (in particular, the clusters[32,33] with $S=2$, recently found to contribute considerably to the low temperature specific heat[34] of $YBa_2Cu_3O_{7-\delta}$), we shall present below an alternative interpretation of the experimental data[11] on the basis of microscopic phase separation in oxygen-deficient 123 superconductors.[9,10,35,36] It is worth reminding here that Eq. (A5) has been derived from Eq. (A1) in the limit of low concentration c of MC acceptors. We will reanalyze the experimental relaxation curves of Tm nuclei without making use of the low concentration limit but employing a computer simulation of the $(M_\infty-M_t)$ curves just on basis of the initial equation (A1). To do so, we make three simplifications. First, we suppose that $TmBCO_{6+x}$ has a tetragonal crystal lattice with parameters $a_0=3.8$ Å and $c_0=3a_0$. Second, we let magnetic centers occupy only either Cu(1) or Cu(2) sites in the lattice. Third, we assume that the relaxation rate

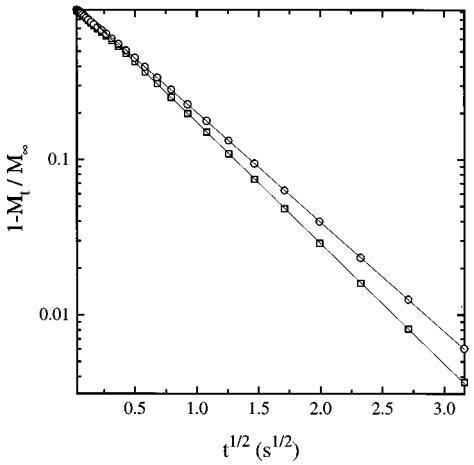

FIG. 4. Computer simulation of the Tm NSLR kinetics in $TmBCO_{6+x}$ containing 1% acceptor magnetic centers at Cu(1) sites. Open squares represent the result of the simplified calculations using the relaxation rate $W \sim r^{-6}$. Open circles are the results obtained by angular averaging of Eq. (A1); solid lines illustrate the $\exp[-(t/T_1)^{1/2}]$ dependences.

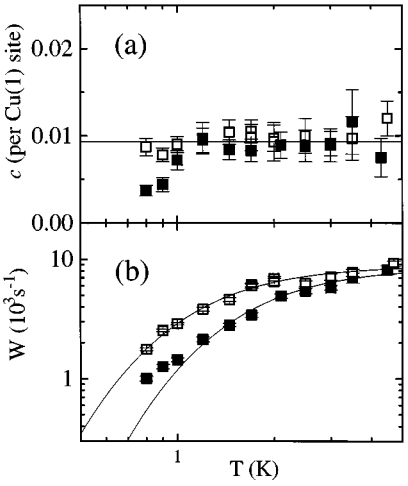

FIG. 5. Tm NSLR parameters for Tm6.6-*qe* as deduced from computer simulations of the recovery curves using Eq. (A1): magnetic centers are located at Cu(1) sites. (a) Concentration c obtained in a primary computer simulation using c and W as free parameters; (b) normalized relaxation rate W obtained in a secondary simulation using the fixed c value of 0.0092 per Cu(1) site. Solid lines in (b) represent the temperature dependence $W \sim [1-\tanh^2(g\mu_B H/2kT)]$. Open squares: 90 MHz, 17.0 kOe, $g=2.0(1)$; solid squares: 125 MHz, 23.6 kOe, $g=2.1(1)$.

$$1/T_1(\vec{r}_j) = (a_0/r_j)^6 W \tag{6}$$

depends only on the Tm-MC distance while calculating Eq. (A1). So, the best fit result of each experimental curve at a given MC-localization type [Cu(1) or Cu(2)] will contain two variables: concentration of magnetic centers c and normalized relaxation probability W [see Eq. (A7)]. In the case of a dipole-dipole interaction for $S=1/2$ one has

$$W = \frac{3}{10} g^2 \mu_B^2 \gamma^2 a_0^{-6} \frac{\tau_c}{1+\omega_0^2 \tau_c^2} \left[1 - \tanh^2 \frac{g\mu_B H_0}{2kT} \right]. \tag{7}$$

Here the averaging of the W angular dependence ($\overline{\sin^2\Theta\cos^2\Theta} = 2/15$) is made. We could have taken into account the angular dependence of the relaxation rate $1/T_1(\vec{r}_j)$, which in the case of ''ordinary'' ^{89}Y-type nuclei is expressed by $\sin^2\Theta\cos^2\Theta$ and is more complicated for Tm nuclei due to the highly anisotropic γ tensor. However, in the case of nonaligned $TmBCO_{6+x}$ powder computer simulations showed the thulium relaxation kinetics calculated from Eqs. (A1) and (6) only slightly differ from the result obtained by angular averaging of Eq. (A1). For example, Fig. 4 shows results of ''exact'' and simplified calculations for the case of MC's localized at Cu(1) sites. As can be seen in Fig. 4, for $t > 0.3T_1$ both curves can be fitted well by $\exp[-(t/T_1)^{1/2}]$, and the difference in T_1 values does not exceed 10%.

Computer simulations for Tm6.6-*qe* show the following. The experimental recovery curves can be fitted by the calculated ones only if the MC's are located at Cu(1) sites. The MC concentration found in this fit [$c = 0.92 \times 10^{-2}$ per unit cell, see Fig. 5(a)] in general agrees with the value 1.3×10^{-2} per unit cell found earlier[16] in experiments with the equilibrium Tm6.6 sample. The W factor at $T=4$ K has a reasonable value [Fig. 5(b)] and at temperature lowering decreases approximately as $[1-\tanh^2(g\mu_B H_0/2kT)]$, the g value being practically the same as $g_\perp$ observed in the Cu^{2+} EPR spectra.[17–19] This result shows that the Tm nuclear relaxation in Tm6.6-*qe* proceeds predominantly via MC's with $S=1/2$ located in the Cu(1) ''chain'' sites.

Similar calculations for Tm6.5-*qe* show that for any MC location [on Cu(1) or Cu(2) sites] a homogeneous random MC distribution in the $TmBCO_{6+x}$ lattice gives the relaxation kinetics of the $\exp[-(t/T_1)^{1/2}]$ type but cannot give the $\exp[-(t/T_1)^{1/3}]$ one, which was observed experimentally and attributed to quasi-2D MC distribution. Much better fits to the experimental Tm relaxation curves (not only in ''quasi-equilibrium'' but also in ''equilibrium'' samples, see Sec. V) are obtained if we allow for an inhomogeneous MC distribution in $TmBCO_{6.5}$, as expected, e.g., in the case of microscopic phase separation in oxygen-deficient 123 compounds.[9,10,35–37] This separation is connected with the tendency of oxygen to order in the CuO_x planes, so that the real crystal lattice of underdoped 123 compounds is represented as a mixture of microdomains with ortho I ($x=1$), ortho II ($0.5<x<0.6$), and tetragonal ($x<0.35$) structures. There is experimental evidence,[9,10,35,36] that the superconductivity of underdoped 123 compounds is provided by a percolative network of mesoscopic platelike ortho I and ortho II domains. The walls of the percolative clusters are enriched by Cu^{2+} paramagnetic centers, which are characterized by slow ($\sim 10^8$ s^{-1}) spin dynamics. Since the size of the SC domains is rather small [the mean size in the b direction varies from $6b_0$ (23 Å) to $13b_0$ (50 Å) at x values ranging from 0.5 to 0.8], the magnetic centers located outside SC domains may have a strong influence on the magnetic relaxation of nuclear probes located inside a SC percolative cluster.

We will use this representation as a starting point and suppose that there are two types of ^{169}Tm nuclei in $TmBCO_{6+x}$: one belonging to the ordered part of the crystal structure, i.e., to the SC clusters which contain a small

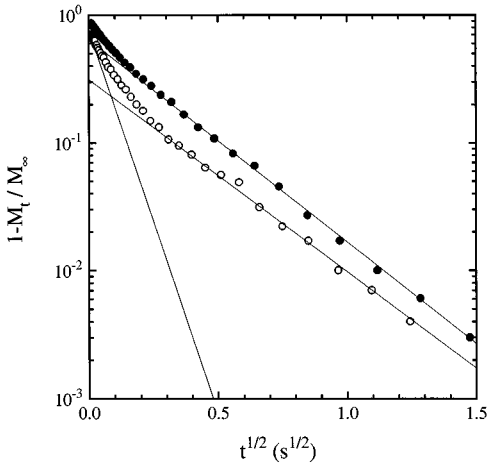

FIG. 6. Tm relaxation kinetics in Tm6.5 (open circles) and Tm6.6 (solid circles) at $\nu=31.55$ MHz, $T=1.4$ K. Drawn lines indicate the initial and final slopes.

amount of MC's, and another one belonging to a disordered part, i.e., tetragonal NSC domains enriched by MC's. Tm nuclei have long relaxation times T_{1o} in the ordered phase and short T_{1d} in the disordered one. If in both phases Tm nuclei and MC's are coupled by dipolar interaction, the experimental Tm relaxation curves in the two phase samples should follow the expression

$$1-M_t/M_\infty = d\exp(-\sqrt{t/T_{1d}})+(1-d)\exp(-\sqrt{t/T_{1o}}), \tag{8}$$

where d is the relative volume fraction of the disordered phase. Figure 6 shows the Tm-magnetization recoveries, Eq. (8), in Tm6.5 and Tm6.6. The results of the best fit of the Tm relaxation curves in Tm6.5-qe measured[11] at 90 MHz between 3–4.5 K give $T_{1d}^{-1}=300\pm100\ \mathrm{s}^{-1}$ and $T_{1o}^{-1}=15\pm5\ \mathrm{s}^{-1}$. At 125 MHz the values are about 1.5 times smaller. As the Tm relaxation rates in the o and d phases differ by a factor 20–30, it means that the effective MC concentration is 5 times larger in the d phase than in the o phase [see Eq. (A10)]. The volume fraction of the d phase is about 50% in the temperature interval 3–4.5 K. At lower temperatures d becomes temperature and field dependent (the higher P_0, the smaller d becomes). This dependence is likely caused by a very strong inhomogeneous broadening in these quasiequilibrium samples, and is not seen in the equilibrium samples discussed in the next section.

The ratio of $T_1^{-1}(90\ \mathrm{MHz})/T_1^{-1}(125\ \mathrm{MHz})\sim1.5$ means [see Eq. (A10)] that $\omega_0\tau_c>1$ and the correlation time $\tau_c<1.8\times10^{-9}$ s. The correlation times in Tm6.5-qe can be determined more precisely (see Fig. 7) from the frequency dependence of the Tm relaxation rates at 4.2 K and appear to be different in the d and o phases:

$$\tau_{cd}=1.7(5)\times10^{-9}\ \mathrm{s}\quad\text{and}\quad\tau_{co}=5.1(8)\times10^{-9}\ \mathrm{s}. \tag{9}$$

Now we can roughly estimate the MC concentration using Eq. (A10). Taking $1/T_{1d}=300\ \mathrm{s}^{-1}$ and $1/T_{1o}=14\ \mathrm{s}^{-1}$ measured at $\nu=90$ MHz and $T=4.5$ K and inserting in Eq. (A10) the values $g=2$ and $\langle\gamma^2\rangle=9.5\times10^8\ \mathrm{Oe}^{-2}\,\mathrm{s}^{-2}$ we obtain $n_d=2.83\times10^{20}\ \mathrm{cm}^{-3}$ and $n_o=6.1\times10^{19}\ \mathrm{cm}^{-3}$, or $n_d=0.046$ and $n_o=0.010$ per unit cell having a volume

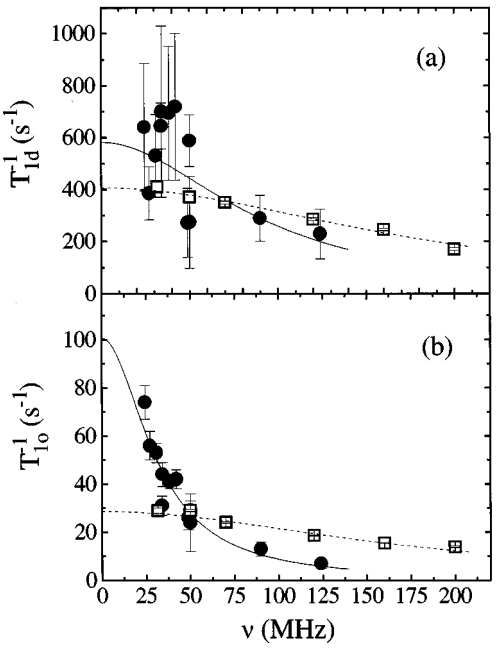

FIG. 7. Frequency dependences $A\cdot\tau_c/(1+\omega^2\tau_c^2)$ of the Tm NSLR rates $1/T_{1d}(1-P_0^2)$ and $1/T_{1o}(1-P_0^2)$ [see Eqs. (8) and (A10)] in Tm6.5-qe (solid circles, solid lines) and in Tm6.5 (open squares, dashed lines) at $T=4.2$ K, $H\perp c$, $H/\nu=0.189$ Oe/kHz. Solid lines correspond to the following parameters: (a) $A=3.5(7)\times10^{11}\ \mathrm{s}^{-2}$, $\tau_c=1.7(5)\times10^{-9}$ s; (b) $A=1.95(7)\times10^{10}\ \mathrm{s}^{-2}$, $\tau_c=5.1(8)\times10^{-9}$ s; the dashed lines to (a) $A=4.73(7)\times10^{11}\ \mathrm{s}^{-2}$, $\tau_c=0.86(3)\times10^{-9}$ s; (b) $A=3.11(2)\times10^{10}\ \mathrm{s}^{-2}$, $\tau_c=0.92(2)\times10^{-9}$ s. The g value of MC's is equal to 2.1.

$\sim3a_0^3=1.65\times10^{-22}\ \mathrm{cm}^3$. The same measurements in the same sample done at $\nu=50$ MHz and $T=1.5$ K after 2 y RTA gave $1/T_{1d}=590\ \mathrm{s}^{-1}$ and $1/T_{1o}=28\ \mathrm{s}^{-1}$ with corresponding values of $n_d=0.047$ and $n_o=0.010$ per unit cell. One can see that the 2 y room-temperature annealing did not change the MC concentrations in both phases. Combining this fact and the behavior of ^{89}Y T_1 vs t_{RTA} (see Sec. III) we conclude that the oxygen ordering in the CuO_x planes has a local nature in quenched samples and is completed after 10 days at room temperature. The changes in the ^{89}Y relaxation after 10 days of RTA are mainly determined by reordering of the charge and spin structure in the CuO_2 planes which are important for nuclear relaxation at temperatures above T_c. For the Tm relaxation measured at low temperatures this reordering in the CuO_2 planes is of minor importance.

V. ^{169}Tm AND ^{63}Cu(1) NUCLEAR RELAXATION IN EQUILIBRIUM $TmBa_2Cu_3O_{6+x}$

As is well known, the most perfect crystal structures and the best parameters (such as narrow SC transitions, narrow Cu NQR lines and so on) are not observed in quenched samples but in those prepared by slow cooling in a proper atmosphere. The degree of oxygen disorder in CuO_x planes is minimal in such samples, so one could expect the MC concentration in equilibrium $TmBCO_{6+x}$ to be smaller than in quenched samples. In this section the results of T_1 measurements for Tm measured by NMR at about 30 MHz and

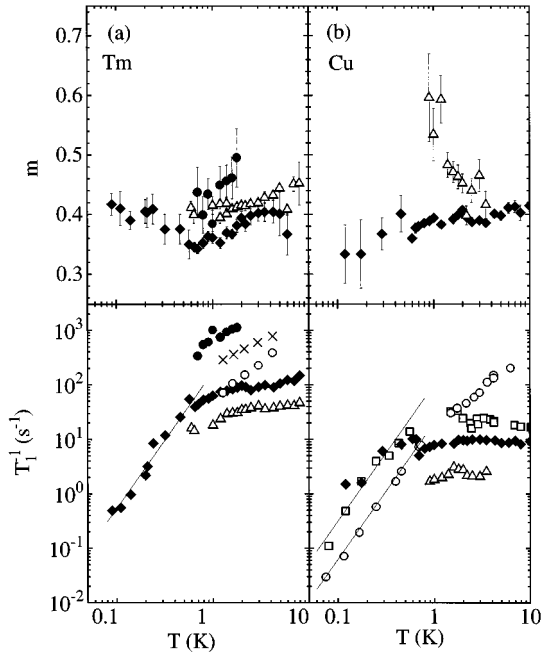

FIG. 8. Tm and twofold coordinated Cu(1) NSLR parameters for well-annealed magnetically aligned $TmBCO_{6+x}$ samples at frequencies of 30.0–31.55 MHz represented on basis of the recovery shape $1-M_t/M_\infty=\exp[-(t/T_1)^m]$. (a) Tm NMR data for $H\|c$, $H=12.3$ kOe; (b) ^{63}Cu(1) NQR data. Open squares, $x=0$; open circles, $x=0.2$; crosses, $x=0.3$; solid circles, $x=0.4$; solid diamonds, $x=0.51$; open triangles, $x=0.6$; solid lines represent the $T^{2.5}$ dependence.

for ''chain'' twofold coordinated ^{63}Cu made by NQR for six $TmBCO_{6+x}$ equilibrium samples with $x=0$, 0.2, 0.3, 0.4, 0.51, and 0.6 are discussed. All experiments for Tm6.4 ($T_c=23$ K), Tm6.5 ($T_c=50$ K), and Tm6.6 ($T_c=55$ K) are performed at 31.55 MHz corresponding to line *A* in the ^{63}Cu(1) NQR spectrum [see Fig. 1(b)]. In order to show the range of T_1 changes with temperature and oxygen content all the results are represented in a unified form using the following description of the relaxation curves:

$$1-M_t/M_\infty=\exp[-(t/T_1)^m]. \tag{10}$$

The main results are displayed in Fig. 8, and can be summarized as follows.

(1) At temperatures above 0.7 K T_1^{-1} of Tm increases with x for $0.2\leqslant x\leqslant 0.4$ and drops sharply for $x>0.4$. This confirms the fact established earlier[8–10] that MC concentration reaches a maximum value at the ''semiconductor-superconductor'' transition ($x=0.4$).

(2) The exponent m for Tm relaxation is near 1/2 for Tm6.4, a little bit less in Tm6.6, and only for Tm6.5 it reaches 1/3 indicating a pseudo-2D character of relaxation. This can simply mean, see Sec. IV, that the effect of microphase separation is most pronounced for Tm6.5, being intermediate between Tm6.4, with a small fraction of the ordered SC phase, and Tm6.6, with a little fraction of disordered NSC phase. In Tm6.5 also the exponent m for Cu(1) nuclei reaches its minimal value.

(3) T_1^{-1} of copper at $T>0.7$ K changes with oxygen content just as T_1^{-1} for thulium, i.e., increases in the range $x<0.4$ and decreases for $x>0.4$. The difference of relaxation rates of thulium and copper for each of Tm6.5 and Tm6.6 samples corresponds roughly to the difference of γ^2 values indicating that above 0.7 K the sources of the fluctuating magnetic fields at the Tm and Cu sites are the same paramagnetic centers coupled with both nuclei by a dipole-dipole interaction.

TABLE I. The mean values of the relaxation parameters for ^{169}Tm and ^{63}Cu(1) in Tm6.4, Tm6.5, and Tm6.6 samples at temperatures 1 K$<T<$6 K.

Sample	Nucleus	Field	T (K)	T_{1d}^{-1} (s^{-1})	T_{1o}^{-1} (s^{-1})	d
Tm6.4	Tm	$H\|\|c$	1–1.5	900	~10	~0.9
		$H\|\|a$	1–1.5	500	~10	~0.9
Tm6.5	Tm	$H\|\|c$	2–6	400	40	0.5
		$H\|\|a$	2–6	320	31	0.5
	Cu(1)	$H=0$	2–6	100	4	0.25
Tm6.6	Tm	$H\|\|c$	2–6	280	22	0.3
	Cu(1)	$H=0$	1–3.5	~100	2	~0.15

(4) The character of relaxation at $T<0.7$ K is quite different: in the Tm6.5 sample the relaxation rates for Tm and Cu(1) become equal at $T\sim 0.25$ K, and at lower temperatures the Cu(1) nuclei relax faster than those of Tm. This indicates a difference in the coupling between the Tm and Cu(1) nuclei with the acceptor magnetic centers and/or changes in the spectral density of fluctuating fields at Tm and Cu(1) sites.

(5) The available experimental data for $T<0.7$ K, namely the temperature dependences of the Cu(1) relaxation rate for Tm6.0, Tm6.2, Tm6.5, and that of Tm for Tm6.5, are fairly well described by $T_1^{-1}=AT^{2.5}$ [straight lines in Figs. 8(a) and 8(b)]. Thus at ultralow temperatures the nuclear relaxation in superconducting Tm6.5 does not differ qualitatively from that in antiferromagnetic Tm6.0 and Tm6.2 compounds. The temperature dependence $T_1^{-1}\sim T^{2.5}$ rules out localized paramagnetic centers as a source of the fluctuating magnetic fields needed for nuclear relaxation.

The quantitative analysis will mainly concern the experimental data for 0.7 K$\leqslant T\leqslant$10 K where the idea of a two-phase superconductor can be used and the distribution of MC's is random and homogeneous in each of two phases. The mean values of the nuclear relaxation parameters in three superconducting samples are given in Table I, and Fig. 9 represents, as an example, the results of the two-exponetial fit of the thulium and copper relaxation curves in Tm6.5 sample. The Tm relaxation parameters shown in Table I indicate that the disordered phase fraction d decreases with x; in Tm6.5 it is equal to 50%, just as in Tm6.5-*qe* one. The same tendency holds for the Cu(1) relaxation, but the d value obtained from the relaxation measurements of Cu(1) in Tm6.5 is equal to 25%. Let us remind the reader that the line *A* of the Cu(1) NQR spectrum [Fig. 1(b)] is believed to account for the copper atoms residing in the ''empty'' Cu-Cu chains with two ''full'' Cu-O-Cu chains as neighbors. If we were dealing only with the ordered ortho II phase, the Cu(1) nuclei at 31.55 MHz should not have exhibited any trace of fast relaxation. The fact that it is nevertheless observed indicates, most likely, that because of the small sizes of the ortho II domains a significant contribution to the NQR signal at 31.55 MHz is provided by the Cu(1) nuclei residing at the

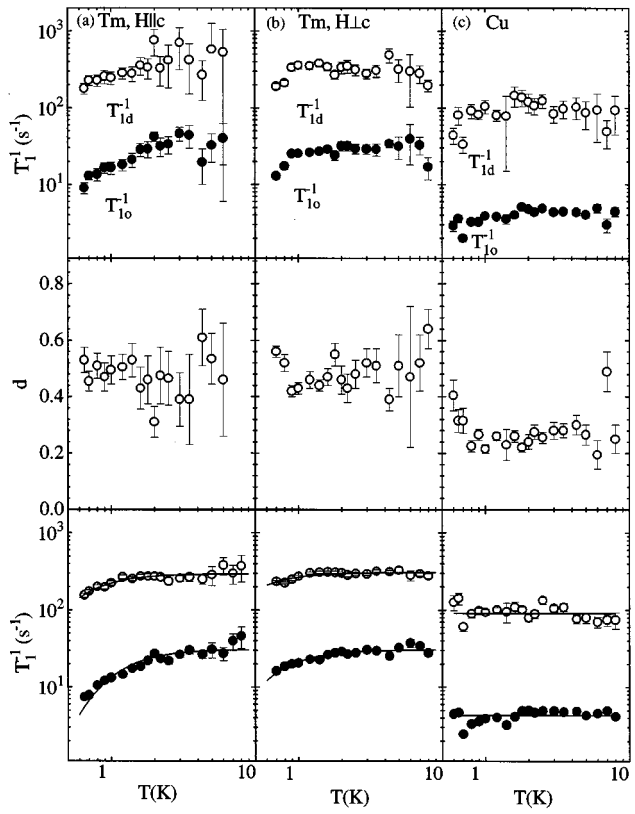

FIG. 9. Tm and Cu(1) NSLR parameters for Tm6.5 at 31.55 MHz as deduced from the decomposition given by Eq. (8). (a) Tm NMR data for $H \| c$, $H=12.3$ kOe; (b) Tm NMR data for $H \perp c$, $H=5.95$ kOe; (c) ^{63}Cu(1) NQR data. Top row, relaxation rates; middle row, d; bottom row, relaxation rates with fixed d (average from middle row). Fits are discussed in the text.

boundaries of the SC clusters, which experience a strong influence of the neighboring d-phase domains. Some contribution to this signal of random combinations of short CuO-chain fragments can also not be ruled out.

The relative volume of the disordered phase as characterized by d, is obtained from the relaxation data of the Tm nuclei. As can be seen from the middle panels of Fig. 9, this parameter for Tm6.5 is T independent. The lower panels of Figs. 9(a) and 9(b) show the T dependence of the relaxation rates for the d and o phases obtained from the experimental $1-M_t/M_\infty$ curves according to Eq. (8) with d fixed at 0.5. Fitting these results with $1/T_1 \sim [1-\tanh^2(g\mu_B H/2kT)]$ gives $g_\parallel^{(d)}=1.3$, $g_\parallel^{(o)}=2.4$, $g_\perp^{(d)}=1.9$, $g_\perp^{(o)}=3.1$. As the experiments are done at low frequency (31.55 MHz), the error in these estimates is quite large due to the sensitivity for small changes in the spin polarization factor and one can speak only about a mean g value. It appears to be equal to 2.2, i.e., confirms the ESR data and points to an effective spin $S=1/2$ for the MC's.

The ^{63}Cu nuclear relaxation rates do not depend on temperature [Fig. 9(c)] because $P_0=0$ in the absence of a magnetic field. The values of the copper nuclear relaxation rates appear to be 3–4 times smaller than those for thulium, while from the $\gamma_{\mathrm{Tm}}^2/\gamma_{\mathrm{Cu}}^2$ ratio a factor $\sim$ 25 times might have been anticipated. However let us notice that the $1/T_1$ value measured at the NQR frequency ($H=0$) is three times larger than the corresponding copper NMR relaxation rate. Besides, in the absence of the external magnetic field terms of B and C type in Eq. (A7) should appreciably contribute to the relaxation rate.

TABLE II. Spin-lattice relaxation parameters of ^{169}Tm and ^{63}Cu(1) for the d and o phases of $TmBCO_{6.51}$ as inferred from computer simulations of the magnetization recovery curves taken at 31.55 MHz. $\langle c_1\rangle$ and $\langle c_2\rangle$ denote the MC concentrations (per Cu atom) for a MC distribution over the Cu(1) and the Cu(2) sublattices, respectively. The normalized relaxation rates W_1 and W_2 are given for $T=4.3$ K, the concentrations $\langle c_1\rangle$ and $\langle c_2\rangle$ are averaged values in the temperature range 0.7 K$<T<$5 K.

Microphase	Nucl.	Field (kOe)	MC's at $\langle c_1\rangle$	Cu(1) W_1 s^{-1}	MC's at $\langle c_2\rangle$	Cu(2) W_2 s^{-1}
d	Tm	12.3($\|\|c$)	0.032	32×10^3	0.026	20×10^3
		5.95($\|\|a$)		38×10^3		33×10^3
	Tm	12.3($\|\|c$)	0.0028	38×10^4	0.0078	21×10^3
o		5.95($\|\|a$)		67×10^4		24×10^3
	$Cu(1)_2$	$H=0$	0.0043	30×10^3	0.0033	25×10^3

Additional evidence that the MC spin is equal to 1/2 is obtained from a computer simulation of the $1-M_t/M_\infty$ relaxation curves following the procedure described in Sec. IV. The results of the simulations with $d_{\mathrm{Tm}}=0.5$ and $d_{\mathrm{Cu}}=0.25$ are shown in Table II. Taking Tm6.5 as example, the simulation of the experimental data obtained for the d phase at 1 K$<T<$5 K, $\nu=31.5$ MHz, $H\perp c$ gives $c_{1d}=0.032$ per Cu(1) or $c_{2d}=0.026$ per Cu(2) site, with a relaxation rate $W=(3.6\pm0.3)\times10^4$ s^{-1}. The normalized Tm nuclear relaxation rate W in a nonaligned powder can also be estimated using Eq. (7). To obtain the values of the correlation time τ_c, we have measured the frequency dependence, Eq. (A10), of the Tm relaxation rates $1/T_{1d}$ and $1/T_{1o}$. The results of these experiments with Tm6.5 at $T=4.2$ K, 31.5 MHz$<\nu<$200 MHz, $H\perp c$ give us the single value $\tau_{cd}=\tau_{co}=0.9(1)\times10^{-9}$ s for both d and o phases, see Fig. 7. A comparison with the correlation times found in Sec. IV for Tm6.5-qe, Eq. (9), shows that the MC spin dynamics in the well-annealed sample is quite different from that in the quenched sample. Taking now the values $\tau_c=0.9(1)\times10^{-9}$ s, $P_0=0$, $S=1/2$, $g=2$, $\langle\gamma^2\rangle=9.5\times10^8$ Oe^{-2} s^{-2} in Eq. (7), we get $W=2.8(3)\times10^4$ s^{-1}. Six of the eight W parameters for Tm in Table II are lying in the interval $(2–4)\times10^4$ s^{-1} which makes it unlikely that S exceeds 1/2.

Our data do not allow a definite choice for Cu(1) or Cu(2) sites as the location of the MC's (see Table II). The MC concentration in the o phase $\langle c\rangle\sim0.003$ is typical for a ''good'' $YBa_2Cu_3O_7$-type superconductor.[4,38] The unusually large W_1 value for Tm nuclei in the o phase could be ascribed to a large spin S for the paramagnetic centers (or clusters) on the Cu(1) sites.[16] It should be noticed, however, that the W and c parameters are interdependent and that the experimental $1-M_t/M_\infty$ curves can be satisfactorily fitted with smaller W values taking a little higher MC concentrations. Actually the c parameter determines the shape of the $1-M_t/M_\infty$ curve, and the probability W, i.e., its time scaling. The appearance of an additional type of MC's with a low concentration[34] should influence first of all the shape of

the $1-M_t/M_\infty$ curves characterizing *the slow relaxation*. The spread in the relaxation parameters for the *o* phase might be partly due to this. To observe the presence of MC's with $S>1/2$, a very high signal-to-noise ratio and a possibility to vary the experimental conditions (the NMR frequency, the magnetic field, and temperature) in a wide range are needed.

VI. CONCLUSIONS

Previous studies on quenched Tm123 samples at temperatures ranging from 4.3 K down to 0.7 K have shown that for the compounds with $x=0.5$ the thulium nuclear relaxation kinetics at $T>2$ K can be fairly well described by Eq. (10) with $m=1/3$. This has been interpreted as a manifestation of quasi-two-dimensional distribution of MC's located in the neighboring CuO_2 planes. The experiments described above, in which the relaxation in a series of well-annealed Tm123 samples was studied in detail, have shown that the peculiar shape of the $1-M_t/M_\infty$ recovery curves in oxygen-deficient 123 compounds is determined by structural inhomogeneities. Computer simulations of the magnetization curves appeared to be very useful. In particular they have shown that a homogeneous random distribution of MC's in the $TmBa_2Cu_3O_{6+x}$ lattice leads to $m=1/2$ but fails in providing the power $m=1/3$ at any type of MC location. The simple relation, Eq. (8), has been found to fit excellently all the nuclear relaxation curves. These results support the idea of a micro-phase separation in oxygen-deficient 123 compounds. Apparently, the 123 samples with $x\geqslant 0.4$ contain hole-poor nonsuperconducting regions (disordered *d* phase) and hole-rich superconducting regions (ordered *o* phase). The nuclei characterized by the short relaxation time T_{1d} can be thought as belonging to droplets of the *d* phase enriched with MC's outside the percolative superconducting clusters of the *o* phase. In the superconducting samples the volume fraction of the *d* phase has a maximum value of 0.85 at $x=0.4$ and decreases steeply as *x* increases. The computer simulations have shown that the relaxation of Tm nuclei in well-annealed $TmBa_2Cu_3O_{6.5}$ at temperatures $T=0.7-10$ K proceeds mainly due to a dipole-dipole interaction with MC's located either at Cu(1) or at Cu(2) sites. The concentration of those MC's having $S=1/2$ and $g=2$ are estimated to be $\sim 3\%$ for the nonsuperconducting *d* phase and $\sim 0.3\%$ for the superconducting *o* phase. For $T<0.7$ K the relaxation rates of both Tm and Cu(1) nuclei in the $x=0.5$ sample decrease as $T^{2.5}$ with temperature lowering down to 75 mK, a power dependence which is also seen in antiferromagnetic $x=0$ and $x=0.2$ compounds. The temperature dependence $1/T_1\sim T^{2.5}$ rules out that localized paramagnetic centers are the channel for nuclear relaxation, and should be studied separately.

ACKNOWLEDGMENTS

This work was supported in part by the Ministry of Science and Technology of Russian Federation, the Scientific Council on HTSC Problem, under Project No. 94029, by the NATO Scientific and Environmental Affairs Division, under Grant Nos. HTECH.930343 and HTECH.LG 950536, and by the Russian Foundation for Basic Research, under Project No. 96-02-17058a.

APPENDIX MAGNETIZATION RECOVERY

Let us consider possible forms of a MC induced recovery of the longitudinal nuclear magnetization $p(t)=1-M_t/M_\infty$ in the absence of nuclear spin diffusion. If a lattice contains N_0 sites, a fraction *c* of which are occupied at random by MC's, the relaxation function has the following form:[14]

$$p(t)=\prod_j \{1-c+c\exp[-t/T_1(\vec{r}_j)]\}, \tag{A1}$$

where $T_1^{-1}(\vec{r}_j)$ is the rate of the relaxation induced by the MC at site *j*. For low *c*, Eq. (A1) transforms into

$$p(t)\approx\exp\left[-N_0 c\int\{1-\exp[-t/T_1(r,\theta)]\}d\vec{r}_D\right]$$
$$=\exp(-R_D n), \tag{A2}$$

where $n=N_0 c$ is the concentration of MC's, *D* is a dimensionality of the system under consideration, $d\vec{r}_D=r^{D-1}drd\Omega_D$. If the nuclei and MC's are coupled by a magnetic dipole-dipole interaction, one has

$$T_1^{-1}(r,\theta)=\alpha r^{-6}f(\Omega), \tag{A3}$$

where $f(\Omega)$ is a function of polar angles defining the orientation of the vector $\vec{r}$ relatively to an external magnetic field, so that

$$R_D=\int[1-\exp(-\alpha r^{-6}f(\Omega)t)]r^{D-1}drd\Omega_D$$
$$=(1/D)(\alpha t)^{D/6}\Gamma(1-D/6)\int f^{D/6}d\Omega_D, \tag{A4}$$

$$p(t)=\exp[-(t/T_1^{(D)})^{D/6}], \tag{A5}$$

$$1/T_1^{(D)}=\alpha\left[(n/D)\Gamma(1-D/6)\int f^{D/6}(\Omega)d\Omega_D\right]^{6/D} \tag{A6}$$

[$\Gamma(a)$ denotes the Γ function]. In general, the direct nuclear relaxation rate due to the spin *S* is defined by the following expression:[14,39]

$$T_1^{-1}(r,\theta)=\frac{2}{3}S(S+1)g^2\mu_B^2\gamma^2 r^{-6}[A+B+C],$$

$$A=\frac{9}{2}\sin^2\theta\cos^2\theta\frac{\tau_c}{1+\omega_0^2\tau_c^2}\frac{\partial B_S(x)}{\partial x},$$

$$B=\frac{1}{4}(1-3\cos^2\theta)^2\frac{\tau_c'}{1+(\omega_S-\omega_0)^2\tau_c'^2}\frac{B_s}{x},$$

$$C=\frac{9}{4}\sin^4\theta\frac{\tau_c'}{1+(\omega_S+\omega_0)^2\tau_c'^2}\frac{B_S}{x}, \tag{A7}$$

where $B_S(x)$ is the Brillouin function, $x=g\mu_B H_0 S/kT$, τ_c and τ_c' are correlation times (usually, spin-lattice and spin-

spin relaxation times of S spins), ω_S and ω_0 are Larmor frequencies of S and I spins, respectively, θ is the angle between vector $\vec{r}$ and an external field $\vec{H}_0$. Under normal experimental conditions one has $(\omega_S \pm \omega_0)^2 \tau_c'^2 \gg 1$, so that Eq. (A7) can be simplified to the following result for $S=1/2$:

$$\alpha = \frac{9}{4} g^2 \mu_B^2 \gamma^2 \frac{\tau_c}{1+\omega_0^2 \tau_c^2}(1-P_0^2), \tag{A8}$$

$$f(\Omega) = \sin^2\theta \cos^2\theta, \tag{A9}$$

where $P_0 = \tanh(g\mu_B H_0/2kT)$ is the polarization factor for the S spins. Combining Eqs. (A8) and (A9) with Eq. (A6) yields, for a three-dimensional system,

$$\frac{1}{T_1^{(3)}} = n^2 \frac{4}{9} \pi^3 g^2 \mu_B^2 \gamma^2 \frac{\tau_c}{1+\omega_0^2 \tau_c^2}(1-P_0^2). \tag{A10}$$

In a particular case of a two-dimensional system the relaxation rate depends on the angle Θ between the external field $\vec{H}_0$ and the normal to the plane containing S and I spins:

$$\frac{1}{T_1^{(2)}} = n^3 \frac{9}{128} \Gamma^3\left(\frac{2}{3}\right) g^2 \mu_B^2 \gamma^2 J^3(\Theta) \frac{\tau_c}{1+\omega_0^2 \tau_c^2}(1-P_0^2). \tag{A11}$$

Here

$$J(\Theta) = 4(2\sin\Theta)^{2/3} \int_0^{\pi/2} [(1-\sin^2\Theta\cos^2\varphi)\cos^2\varphi]^{1/3} d\varphi, \tag{A12}$$

and ensemble averaging is taken over all possible angles φ between the projection $\vec{H}_0$ onto the plane and the vectors connecting the nucleus and the paramagnetic centers. If the field $\vec{H}_0$ lies in the plane, then

$$\frac{1}{T_1^{(2)}} = n^3 \left(\frac{3}{2}\right)^5 \Gamma^6\left(\frac{5}{6}\right) g^2 \mu_B^2 \gamma^2 \frac{\tau_c}{1+\omega_0^2 \tau_c^2}(1-P_0^2). \tag{A13}$$

In addition to the relaxation via MC's, an independent relaxation channel for nuclei may exist (for example, due to conduction electrons in a metal). In this case the magnetization recovery has a general form:

$$1 - M_t/M_\infty = \exp[-(t/T_1^{(D)})^{D/6}] \exp(-t/T_1'). \tag{A14}$$

*During this work also at Leiden.
†During this work also at Orsay.

[1] A. Abragam and B. Bleaney, *Electron Paramagnetic Resonance of Transition Ions* (Clarendon Press, Oxford, 1970).
[2] J. Sichelschmidt, B. Elschner, A. Loidl, and K. Fischer, Z. Phys. B **93**, 407 (1994).
[3] P. Simon, J.M. Bassat, S.B. Oseroff, Z. Fisk, S-W. Cheong, A. Wattiaux, and Sheldon Schultz, Phys. Rev. B **48**, 4216 (1993).
[4] N.E. Phillips, J.P. Emerson, R.A. Fischer, J.E. Gordon, B.F. Woodfield, and D.A. Wright. J. Supercond. **7**, 251 (1994).
[5] A. Abragam and M. Goldman, *Nuclear Magnetism: Order and Disorder* (Clarendon Press, Oxford, 1982).
[6] O.N. Bakharev, A.V. Dooglav, A.V. Egorov, H. Lütgemeier, M.P. Rodionova, M.A. Teplov, A.G. Volodin, and D. Wagener, Appl. Magn. Res. **3**, 613 (1992).
[7] A. Abragam and B. Bleaney, Proc. R. Soc. A **387**, 221 (1983); L.K. Aminov and M.A. Teplov, Sov. Phys. Usp. **28**, 762 (1985).
[8] O.N. Bakharev, A.G. Volodin, A.V. Dooglav, A.V. Egorov, O.B. Marvin, V.V. Naletov, M.A. Teplov, and D. Wagener, JETP Lett. **58**, 608 (1993).
[9] O.N. Bakharev, A.V. Dooglav, A.V. Egorov, O.B. Marvin, V.V. Naletov, M.A. Teplov, A.G. Volodin, and D. Wagener, in *Phase Separation in Cuprate Superconductors*, edited by E. Sigmund and K.A. Muller (Springer-Verlag, Berlin, 1994), p. 257.
[10] M.A. Teplov, O.N. Bakharev, A.V. Dooglav, A.V. Egorov, E.V. Krjukov, O.B. Marvin, V.V. Naletov, A.G. Volodin, and D. Wagener, Physica C **235-240**, 265 (1994).
[11] O.N. Bakharev, J. Witteveen, H.B. Brom, E.V. Krjukov, O.B. Marvin, and M.A. Teplov, Phys. Rev. B **51**, 693 (1995).
[12] M.A. Teplov, A.V. Dooglav, E.V. Krjukov, O.B. Marvin, I.R. Mukhamedshin, and D. Wagener, JETP **82**, 370 (1996).
[13] D. Tse, S.R. Hartmann, Phys. Rev. Lett. **21**, 511 (1968).
[14] M.R. McHenry, B.G. Silbernagel, and J.H. Wernick, Phys. Rev. B **5**, 2958 (1972).
[15] A.V. Egorov, H. Lütgemeier, D. Wagener, A.V. Dooglav, and M.A. Teplov, Solid State Commun. **83**, 111 (1992).
[16] M.A. Teplov, O.N. Bakharev, H.B. Brom, A.V. Dooglav, A.V. Egorov, E.V. Krjukov, O.B. Marvin, I.R. Mukhamedshin, V.V. Naletov, A.G. Volodin, D. Wagener, and J. Witteveen, J. Superconduct. **8**, 413 (1995).
[17] D. Shaltiel, H. Bill, P. Fischer, M. Francois, H. Hagemann, M. Peter, Y. Ravisekhar, W. Sadowski, H.J. Scheel, G. Triscone, E. Walker, and K. Yvon, Physica C **158**, 424 (1989).
[18] J. Stankowski, W. Hilczer, J. Baszynski, B. Czyzak, and L. Szczepanska. Solid State Commun. **77**, 125 (1991).
[19] I.A. Garifullin, N.N. Garif'yanov, N.E. Alekseevskii, and S.F. Kim, Physica C **179**, 9 (1991).
[20] A.V. Dooglav, H. Alloul, M.V. Eremin, and A.G. Volodin, Physica C **272**, 242 (1996).
[21] H.A. Hoff, L.E. Toth, M.E. Filipkowski, C.L. Vold, S.H. Lawrense, R.A. Masumura, W.L. Lechter, and D.K. Smith, J. Electron. Mater. **22**, 1241 (1993).
[22] J.L. Routbort and S.J. Rothman, J. Appl. Phys. **76**, 5615 (1994).
[23] T. Graf, G. Triscone, and J. Muller, J. Less-Common Met. **159**, 349 (1990).
[24] I. Heinmaa, H. Lütgemeier, S. Pekker, G. Krabbes, and M. Buchgeister, Appl. Magn. Res. **3**, 689 (1992).
[25] B.W. Veal, A. Paulikas, Hoydoo You, Hao Shi, Y. Fang, and J.W. Downey, Phys. Rev. B **42**, 6305 (1990).
[26] J.D. Jorgensen, Shiyou Pei, P. Lightfoot, Hao Shi, A.P. Paulikas, and B.W. Veal, Physica C **167**, 571 (1990).
[27] F.C. Chou, F. Borsa, J.H. Cho, D.C. Johnston, A. Lascialfari, D.R. Torgeson, and J. Ziolo, Phys. Rev. Lett. **71**, 2323 (1993).
[28] H. Alloul, A. Mahajan, H. Casalta, and O. Klein, Phys. Rev. Lett. **70**, 1171 (1993).
[29] C. Picard and P. Gerdanian, Physica C **196**, 297 (1992).
[30] E.V. Krjukov, O.B. Marvin, E.A. Semenova, M.A. Teplov, K.M.

Enikeev, and A.V. Klochkov, JETP Lett. **60**, 30 (1994).
[31] S. Semenovskaya and A.G. Khachaturyan, Phys. Rev. B **46**, 6511 (1992).
[32] M.V. Eremin and E. Sigmund, Solid State Commun. **90**, 795 (1994).
[33] O.N. Bakharev, M.V. Eremin, and M.A.Teplov, JETP Lett. **61**, 515 (1995).
[34] J.P. Emerson, D.A. Wright, R.A. Fisher, and N.E. Phillips, *Proceedings of LT-21* [Czech. J. Phys. **46**, 1209 (1996)].
[35] J. Mesot, P. Allenspach, U. Staub, A. Furrer, and H. Mutka, Phys. Rev. Lett. **70**, 865 (1993).
[36] M. Iliev, C. Thomsen, J. Kircher, and M. Cardona. Phys. Rev. B **47**, 12 341 (1993).
[37] L.K. Aminov, B.Z. Malkin and M.A. Teplov, in *Handbook on the Physics and Chemistry of Rare Earths*, edited by K.A. Gschneidner, Jr. and L. Eyring (Elsevier Science, Amsterdam, 1996), Vol. 22, Chap. 150, p. 295.
[38] W.C. Lee, K. Sun, L.L. Miller, D.C. Johnston, R.A. Klemm, S. Kim, R.A. Fischer, and N.E. Phillips, Phys. Rev. B **43**, 463 (1991).
[39] I.J. Lowe and D. Tse, Phys. Rev. **166**, 279 (1968).